Article

Unveiling the Complexity of HIV Transmission: Integrating Multi-Level Infections via Fractal-Fractional Analysis

Yasir Nadeem Anjam [1,*], Rubayyi Turki Alqahtani [2], Nadiyah Hussain Alharthi [2] and Saira Tabassum [1]

[1] Department of Applied Sciences, National Textile University, Faisalabad 37610, Pakistan; tabassumsaira92@gmail.com
[2] Department of Mathematics and Statistics, College of Science, Imam Mohammad Ibn Saud Islamic University (IMSIU), Riyadh 11623, Saudi Arabia; rtalqahtani@imamu.edu.sa (R.T.A.); nhalharthi@imamu.edu.sa (N.H.A.)
[*] Correspondence: ynanjam@ntu.edu.pk

Abstract: This article presents a non-linear deterministic mathematical model that captures the evolving dynamics of HIV disease spread, considering three levels of infection in a population. The model integrates fractal-fractional order derivatives using the Caputo operator and undergoes qualitative analysis to establish the existence and uniqueness of solutions via fixed-point theory. Ulam-Hyer stability is confirmed through nonlinear functional analysis, accounting for small perturbations. Numerical solutions are obtained using the fractional Adam-Bashforth iterative scheme and corroborated through MATLAB simulations. The results, plotted across various fractional orders and fractal dimensions, are compared with integer orders, revealing trends towards HIV disease-free equilibrium points for infective and recovered populations. Meanwhile, susceptible individuals decrease towards this equilibrium state, indicating stability in HIV exposure. The study emphasizes the critical role of controlling transmission rates to mitigate fatalities, curb HIV transmission, and enhance recovery rates. This proposed strategy offers a competitive advantage, enhancing comprehension of the model's intricate dynamics.

Keywords: HIV model; fractal-fractional derivative; existence and uniqueness; Ulam-Hyers stability; fractional Adams-Bashforth method; numerical simulation

1. Introduction

HIV, the human immunodeficiency virus, gradually weakens the immune system, leading to Acquired Immune Deficiency Syndrome (AIDS), where the immune system is compromised [1]. Transmission occurs through various modes such as sexual contact, needle sharing among drug users, vertical transmission from mother to child, and contaminated blood transfusions [2,3]. Understanding the dynamics of HIV transmission is crucial for developing effective prevention and treatment strategies. Mathematical modeling plays a key role in providing insights into virus epidemiology, forecasting trends, evaluating interventions, and addressing critical social issues. While traditional epidemiological compartmental models demonstrate regularity, global challenges often show quasi-linear characteristics, necessitating non-linear mathematical models for precise explanations [4,5]. Studies on HIV transmission dynamics have explored factors like viral load, transmission routes, and demographics, integrating pre-exposure prophylaxis and treatment strategies [6,7]. Mathematical methods also inform clinical guidelines for HIV/AIDS diagnosis, monitoring, and treatment [8]. Furthermore, research has focused on modeling and controlling HIV/AIDS transmission in China using real data from 2004 to 2016 [9], analyzing the stability of infection-age structured HIV-1 models that connect within-host and between-host dynamics [10], developing peptide inhibitors for HIV transmission [11], creating mathematical models of HIV transmission and infection dynamics [12], understanding the dynamics of HIV/AIDS transmission concerning protection awareness and fluctuations [13], conducting numerical investigations of stochastic HIV/AIDS infection models [14], exploring

global dynamics of age-infection HIV models with a nonlinear infection rate [15], and modeling epidemic dynamics of HIV/AIDS transmission with different latent stages based on treatment [16]. Additionally, [17] developed an epidemic model for HBV infection, incorporating vaccination and medication administered through hospitalization.

Recent studies have introduced fractional calculus as a powerful tool for dealing with derivatives and integrals of any positive real order, enhancing models with non-local characteristics and memory dependencies [18]. Fractional techniques like Riemann-Liouville, Hadamard, Katugampola, and Caputo derivatives have significantly improved the accuracy of simulating real-world phenomena. The concept of fractional derivatives was first introduced by Riemann-Liouville in 1832, with Caputo later refining it in 1967 to incorporate boundary and initial conditions for more practical problem-solving in real-world contexts [19,20]. Numerical, computational, and iterative methods have been used to investigate fractional-order mathematical models. Caputo and Fabrizio invented the Caputo-Fabrizio (CF) derivative to overcome the limitations of the classic Caputo operator. This derivative increases exactness under specific situations and resolves problems with singular kernels [21–23]. Caputo further extended Atangana-Baleanu fractional derivatives and incorporated the Mittag-Leffler function from the Caputo-Fabrizio derivative [24]. They developed a fractional mathematical model for Atangana-Baleanu Caputo derivatives based on the Caputo-Fabrizio operator. Conversely, [25] explored the mathematical modeling of COVID-19 with the Caputo-Fabrizio operator. Each operator is tailored to specific systems based on their features and the desired degree of flexibility.

Atangana's recent research delves into the intricate relationship between fractional and fractal mathematics, introducing a novel fractal-fractional operator characterized by both self-similarity and fractional calculus properties [24]. An operator with a degree of self-similarity or fractal-like behavior combined with operations exhibiting fractional calculus qualities is called a fractal-fractional operator. These operators find utility in mathematical models aimed at describing complex and non-linear phenomena characterized by memory effects or patterns that repeat at varying scales. This field of research holds great potential for addressing a variety of challenging issues in diverse settings. Interestingly, this operator offers a more efficient method for extracting fractal fractions compared to conventional techniques, as it captures both the fractional order and the fractal dimension [26,27]. Fractal-fractional derivatives offer a unique approach to exploring fractional operators and fractal dimensions concurrently, enabling the development of models that effectively capture memory effects in dynamic systems. Moreover, researchers have leveraged alternative kernels and fractal-fractional differential equations to address challenges within the domain of fractal-fractional differential equations [28]. Fractional calculus has garnered significant attention from the global scientific community, thanks to its diverse features and practical applications across physics and engineering. It is essential to use a fractional-order system model to observe memory, crossover behavior, and hereditary features in systems [29]. This operator enables more effective modeling of complex systems with memory-dependent dynamics, finding applications in health surveillance and COVID-19 modeling. Studies by Qureshi [30], Li [31], Owolabi [32], Ahmad [33], Anjam [34], Liu [35], and Ahmad [36] demonstrate the utility of fractal-fractional operators across diverse fields. Qureshi and Atangana [37] have investigated models of nonlinear diarrhea transmission dynamics employing fractal-fractional operators. Furthermore, novel fractal-fractional operators have been applied to study the propagation of COVID-19, examining the effectiveness of lockdowns and vaccination strategies in controlling disease transmission [38]. Farman [39] suggests a compound-fractal methodology for modeling plant virus dynamics.

The choice of a fractional operator, coupled with its specific kernel type, plays a critical role in accurately portraying the memory effects, crossover behavior, and long-term dynamics inherent in models of HIV disease transmission. Selecting the Caputo operator with a power law kernel is particularly essential due to its capacity to effectively capture these memory effects and long-range dependencies within the system. These attributes are vital for modeling the intricate transmission dynamics of HIV disease, as they allow

for a detailed depiction of the multifaceted interactions among various factors influencing the virus's spread. These factors encompass healthcare policies, societal perceptions, individual behaviors, and the efficacy of interventions, all of which significantly contribute to understanding and managing HIV transmission dynamics. These insights have guided the research in highlighting the broad significance of its discoveries.

This study explores the dynamics of HIV disease transmission, focusing on three infection levels within a population. The developed model incorporates a fractal-fractional order derivative with a power law kernel and conducts stability analysis through a nonlinear deterministic HIV transmission model. The model classifies the population into five mutually inclusive classes: susceptible individuals, different stages of infection, and recovered individuals. The analysis includes a thorough examination to validate the model's reliability, confirming the existence and uniqueness of solutions within the fixed-point theory framework. Subsequently, Ulam-Hyres stability is applied using nonlinear functional analysis to verify solution stability. Recognizing the significance of the topic, a novel fractional Adam-Bashforth iterative numerical scheme is employed for numerical simulations, with results validated through MATLAB simulations. The numerical results are graphically represented for various fractional orders and fractal dimensions, facilitating comparisons with integer orders. The study highlights the sensitivity of adjusting the fractional order and fractal dimension, emphasizing the practicality of the fractional approach.

The structure of the work is delineated as follows: Section 2 provides an overview of the model's development and rationale. Section 3 delves into the analytical foundations of the techniques employed. The fractional representation of the developed model is expounded upon in Section 4. Section 5 is dedicated to establishing the existence and uniqueness within the fixed-point theory framework, alongside addressing stability analysis. Details of the numerical simulations conducted using the fractional Adams-Bashforth method to validate the theoretical findings are presented in Section 6. MATLAB (ver. 2023b) is also leveraged for numerical simulations to visually represent the results. Lastly, the concluding section encapsulates the key findings of the proposed model.

2. Development of the Model

Model Description

Mathematical models are essential for comprehending the dynamics of HIV transmission and for crafting efficient prevention and treatment strategies. Employing epidemiological methods in constructing these models is crucial to illuminating the underlying mechanisms of HIV transmission. Identifying key determinants is essential for controlling the spread of HIV. Various HIV transmission models, grounded in infectious mechanisms, have been developed and documented, significantly contributing to the design of prevention and treatment strategies. These models play a pivotal role in addressing the HIV epidemic [7,8].

This study is centered on investigating a mathematical model to understand the transmission dynamics of HIV disease within a population, encompassing three levels of infection. The mathematical model divides the whole population $\mathcal{N}(\xi)$ into five subsets: susceptible individuals $\mathcal{S}(\xi)$, individuals at infective stage 1 $\mathcal{I}_1(\xi)$, individuals at infective stage 2 $\mathcal{I}_2(\xi)$, individuals under treatment $\mathcal{Q}(\xi)$, and recovered individuals $\mathcal{R}(\xi)$. Thus, the total human population at any time ξ is represented as:

$$\mathcal{N}(\xi) = \mathcal{S}(\xi) + \mathcal{I}_1(\xi) + \mathcal{I}_2(\xi) + \mathcal{Q}(\xi) + \mathcal{R}(\xi).$$

This arrangement enables us to capture the dynamics of the HIV model by integrating three levels of infection. This is achieved by monitoring the transitions between these

distinct states within the population over time. Thus, the fundamental transmission dynamic model of HIV spread in the human population can be summarized as follows:

$$
\begin{aligned}
\frac{d\mathcal{S}}{d\xi} &= \Lambda - \mu\mathcal{S} - (\beta_1\mathcal{I}_1 + \beta_2\mathcal{I}_2)\mathcal{S}, \\
\frac{d\mathcal{I}_1}{d\xi} &= \beta_1\mathcal{I}_1\mathcal{S} + \delta_2\mathcal{I}_2 - \delta_1\mathcal{I}_1 - \gamma_1\mathcal{I}_1 - \mu\mathcal{I}_1 - \sigma_1\mathcal{I}_1, \\
\frac{d\mathcal{I}_2}{d\xi} &= \beta_2\mathcal{I}_2\mathcal{S} + \delta_4\mathcal{Q} + \delta_1\mathcal{I}_1 - \gamma_2\mathcal{I}_2 - \delta_2\mathcal{I}_2 - \delta_3\mathcal{I}_2 - \mu\mathcal{I}_2 - \sigma_2\mathcal{I}_2, \\
\frac{d\mathcal{Q}}{d\xi} &= \delta_3\mathcal{I}_2 - \gamma_3\mathcal{Q} - \delta_4\mathcal{Q} - \mu\mathcal{Q} - \sigma_3\mathcal{Q}, \\
\frac{d\mathcal{R}}{d\xi} &= \sigma_1\mathcal{I}_1 + \sigma_2\mathcal{I}_2 + \sigma_3\mathcal{Q} - \mu\mathcal{R},
\end{aligned}
\tag{1}
$$

regarding the initial data set:

$$
\mathcal{S}(0) \geq 0, \ \ \mathcal{I}_1(0) \geq 0, \ \ \mathcal{I}_2(0) \geq 0, \ \ \mathcal{Q}(0) \geq 0, \ \ \mathcal{R}(0) \geq 0.
$$

The system (1) comprises several dependent parameters, each with detailed descriptions as follows: Λ denotes the recruitment rate of the population, β_1 represents the transmission coefficient from susceptible individuals to infected individuals in stage 1, β_2 is the transmission coefficient from susceptible individuals to infected individuals in stage 2, μ is the natural death rate for each compartment, δ_1 measures the rate of transmission from infected individuals in stage 1 to those in stage 2, δ_2 denotes the rate of transmission from infected individuals in stage 2 to those in stage 1, δ_3 represents the rate of transmission from infected individuals in stage 2 to those hospitalized, and δ_4 is the rate at which hospitalized patients transition to infected individuals in stage 2. Additionally, σ_1, σ_2 and σ_3 are the coefficients of transmission for infected individuals in stage 1, stage 2, and hospitalized cases transitioning to recovered cases, respectively. Finally, γ_1, γ_2, and γ_3 indicate the death rate of infected individuals in stage 1, stage 2, and hospitalized cases, respectively.

3. Basic Preliminaries

In this section, our objective is to explore our proposed model further by revisiting various essential concepts, definitions, and lemmas.

Definition 1 ([24])**.** *Suppose $\eta(\xi)$ is a function that is differentiable. The expression for the fractal-fractional derivative with fractional order $0 < \alpha \leq 1$ and fractal dimension $0 < \beta \leq 1$ can be formulated as follows:*

$$
^{\mathcal{FF}}\mathbf{D}_\xi^{\alpha,\beta}(\eta(\xi)) = \frac{1}{(q-\alpha)}\frac{d}{d\xi^\beta}\int_0^\xi (\xi-x)^{q-\alpha-1}\eta(x)dx,
$$

including $q - 1 < \alpha$, $\beta \leq q$, where $q \in \mathbb{N}$ and $\frac{d\eta(x)}{dx^\beta} = \lim_{\xi \to 0}\frac{\eta(\xi)-\eta(x)}{\xi^\beta - x^\beta}$.

Definition 2 ([24])**.** *If $\eta(\xi)$ is a continuous function, the integral of fractal-fractional order incorporating the function $\eta(\xi)$ with order α can be represented as follows:*

$$
^{\mathcal{FF}}\mathbf{I}^\alpha\eta(\xi) = \frac{\beta}{\Gamma(\alpha)}\int_0^\xi (\xi-x)^{\alpha-1}x^{\beta-1}\eta(x)dx.
$$

Definition 3. *The integral with a fractional order, specifically the Caputo derivative, associated with the function η, can be described as follows:*

$$
\mathbf{I}_\xi^\alpha\eta(\xi) = \frac{1}{\Gamma(\alpha)}\int_0^\xi (\xi-x)^{1-\alpha}\eta(x)dx, \ \ \xi > 0.
$$

Definition 4 ([40] Contraction Mapping). *Suppose $\mathcal{B}$ is a Banach space. The operator $\mathcal{P}$, which maps from* **X** *to* **X***, is a contraction if and only if:*

$$\|\mathcal{P}(x) - \mathcal{P}(y)\| \leq \mathcal{W}\|x - y\|, \quad \forall x, y, \in \mathbf{X}, 0 < \mathcal{W} < 1.$$

Lemma 1 ([40] Banach's Fixed Point Theorem). *In a Banach space $\mathcal{B}$, when considering a non-empty open subset Ω, a contraction mapping q onto Ω has a unique fixed point.*

Lemma 2 ([40] Krasnoselskii's Fixed Points Theorem). *Within the Banach space $\mathcal{B}$, there is a non-empty, closed, convex subset Ω. Let's consider two operators, denoted as $\mathcal{P}_1$ and $\mathcal{P}_2$, which satisfy the following conditions:*

(i) $\mathcal{P}_1 x + \mathcal{P}_2 y \in \Omega, \forall x, y \in \Omega$,
(ii) *There is a compact and continuous operator $\mathcal{P}_1$,*
(iii) *A contraction mapping is defined by $\mathcal{P}_2$.*

Then, there exists $z \in \Omega$ which is equal to $\mathcal{P}_1 z + \mathcal{P}_2 z = z$.

Corollary 1 ([41]). *Suppose $\mathcal{Y}(\xi) \in \mathbb{C}(r_1, r_2)$ and ${}^{\mathcal{FF}}\mathbf{D}_\xi^\alpha(\eta(\xi)) \in \mathbb{C}(r_1, r_2)$ where $\alpha \in (0, 1]$. If:*

(i) ${}^{\mathcal{FF}}\mathbf{D}_\xi^\alpha(\eta(\xi)) \geq 0$ *for all $\xi \in (r_1, r_2)$, hence, $\mathcal{Y}(\xi)$ does not decrease.*
(ii) ${}^{\mathcal{FF}}\mathbf{D}_\xi^\alpha(\eta(\xi)) \leq 0$ *for all $\xi \in (r_1, r_2)$, hence, $\mathcal{Y}(\xi)$ does not increase.*

Theorem 1 ([42]). *In a metric space that is complete, every sequence that contracts converges as a Cauchy sequence within that space.*

Theorem 2 ([42]). *Suppose $A \subseteq \mathbb{R}$ and $\varsigma : A \to \mathbb{R}^n$ are mappings that are continuously differentiable, with s belonging to A. For every compact subset $\mathcal{A}$ of A, the mapping ς obeys a Lipschitz condition with a Lipschitz constant denoted as L, where $L > 0$ signifies the supremum of the derivative of ς over $\mathcal{A}$, expressed as:*

$$L = \sup_{s \in \mathcal{A}} \left| \frac{d\varsigma}{ds} \right|.$$

4. Fractional Formulation of the Proposed Model

Traditional models using integer-order derivatives often struggle to capture the intricate and dynamic behavior of disease propagation with the robustness and efficiency required for accurate analysis. In contrast, fractional-order models offer a more suitable framework for analyzing real-world data and providing a detailed description of complex occurrences. In the modeling of HIV spread as outlined in system (1), we opted to replace the traditional integer-order time derivative D_t with the fractal-fractional order derivative ${}^{\mathcal{FF}}\mathbf{D}$. This choice of fractional order allows us to capture memory effects and gain a more profound understanding of the disease dynamics.

Additionally, the integer-order model (1) for HIV transmission dynamics is inherently complex and nonlinear, lacking memory effects common in many complex biological systems. This memory effect is crucial for capturing the lasting impact of past infections on the current spread of the virus. To address this limitation, we employ the concept of general fractional operators (as discussed in Section 3) in the HIV spreading model. Fractional derivatives inherently possess a hereditary property, making them suitable for modeling a wider range of real-world phenomena beyond classical integer-order systems with derivatives ranging between 0 and 1. In this study, we employ a system of nonlinear fractional-order equations utilizing the fractal-fractional derivative in the Caputo sense. Previous research indicates that the Caputo derivative, utilizing the power-law kernel, is adept at modeling power-law processes encountered in real-world scenarios. By replacing the time derivative with the Caputo derivative and utilizing a numerical scheme, we incorporate the power law effect inherent in fractional calculus. This methodology enables the model to generate numerical results for different fractional values, depicting the

system's dynamics near the steady-state condition. Integrating fractional-order derivatives ensures that the resulting model accurately reflects the underlying dynamics of HIV transmission, including both short-term and long-term infection rate effects. This adaptability enables a closer alignment with observed data and a more nuanced understanding of the fundamental mechanisms driving HIV transmission. Therefore, these modifications and extensions are applied to the deterministic mathematical model (1) for the HIV epidemic, incorporating various infection stages. Consequently, the revised fractional HIV epidemic model is expressed as follows:

$$
\begin{aligned}
{}^{\mathcal{FF}}\mathbf{D}^{\alpha,\beta}\mathcal{S} &= \Lambda - \mu\mathcal{S} - (\beta_1\mathcal{I}_1 + \beta_2\mathcal{I}_2)\mathcal{S}, \\
{}^{\mathcal{FF}}\mathbf{D}^{\alpha,\beta}\mathcal{I}_1 &= \beta_1\mathcal{I}_1\mathcal{S} + \delta_2\mathcal{I}_2 - \delta_1\mathcal{I}_1 - \gamma_1\mathcal{I}_1 - \mu\mathcal{I}_1 - \sigma_1\mathcal{I}_1, \\
{}^{\mathcal{FF}}\mathbf{D}^{\alpha,\beta}\mathcal{I}_2 &= \beta_2\mathcal{I}_2\mathcal{S} + \delta_4\mathcal{Q} + \delta_1\mathcal{I}_1 - \gamma_2\mathcal{I}_2 - \delta_2\mathcal{I}_2 - \delta_3\mathcal{I}_2 - \mu\mathcal{I}_2 - \sigma_2\mathcal{I}_2, \\
{}^{\mathcal{FF}}\mathbf{D}^{\alpha,\beta}\mathcal{Q} &= \delta_3\mathcal{I}_2 - \gamma_3\mathcal{Q} - \delta_4\mathcal{Q} - \mu\mathcal{Q} - \sigma_3\mathcal{Q}, \\
{}^{\mathcal{FF}}\mathbf{D}^{\alpha,\beta}\mathcal{R} &= \sigma_1\mathcal{I}_1 + \sigma_2\mathcal{I}_2 + \sigma_3\mathcal{Q} - \mu\mathcal{R},
\end{aligned}
\tag{2}
$$

with the initial condition

$$
\mathcal{S}(0) = \mathcal{S}_0 \geq 0, \ \ \mathcal{I}_1(0) = \mathcal{I}_{10} \geq 0, \ \ \mathcal{I}_2(0) = \mathcal{I}_{20} \geq 0, \ \ \mathcal{Q}(0) = \mathcal{Q}_0 \geq 0, \ \ \mathcal{R}(0) = \mathcal{R}_0 \geq 0.
$$

5. Exploring Theoretical Aspects of the Proposed Model

In this section, we conduct a comprehensive examination of the formulated model, delving into its fundamental characteristics and confirming its appropriateness for numerical approximations. To ensure the model's reliability, we validate the existence and uniqueness of its solution using the definitions and theorems referenced in [24]. This rigorous theoretical analysis provides insights into the model's behavior and confirms the feasibility of conducting rigorous numerical experiments.

Let's consider the existence of model (1). We define a Banach space $\mathcal{B} = \mathbf{X} \times \mathbf{X} \times \mathbf{X} \times \mathbf{X} \times \mathbf{X}$, where $\mathbf{X} = (\mathcal{C}[0,T], \mathbb{R})$, with a norm defined as a set of values representing a function space. The function space is denoted by $\|\Xi\| = \max_{\xi\in[0,T]} |\Xi(\xi)|$. Specifically,

$$
\|\Xi\| = \|\mathcal{S}, \mathcal{I}_1, \mathcal{I}_2, \mathcal{Q}, \mathcal{R}\| = \max_{\xi\in[0,T]}\left\{|\mathcal{S}(\xi)| + |\mathcal{I}_1(\xi)| + |\mathcal{I}_2(\xi)| + |\mathcal{Q}(\xi)| + |\mathcal{R}(\xi)|\right\}.
$$

Next, it is essential to compute the specified integral. This leads to the following expression for the right-hand side of model (1):

$$
\begin{aligned}
{}^{\mathcal{RL}}\mathbf{D}^{\alpha}\mathcal{S}(\xi) &= \beta\xi^{\beta-1}G_1(\mathcal{S}, \mathcal{I}_1, \mathcal{I}_2, \mathcal{Q}, \mathcal{R}, \xi) = \Lambda - \mu\mathcal{S} - (\beta_1\mathcal{I}_1 + \beta_2\mathcal{I}_2)\mathcal{S}, \\
{}^{\mathcal{RL}}\mathbf{D}^{\alpha}\mathcal{I}_1(\xi) &= \beta\xi^{\beta-1}G_2(\mathcal{S}, \mathcal{I}_1, \mathcal{I}_2, \mathcal{Q}, \mathcal{R}, \xi) = \beta_1\mathcal{I}_1\mathcal{S} + \delta_2\mathcal{I}_2 - \delta_1\mathcal{I}_1 - \gamma_1\mathcal{I}_1 - \mu\mathcal{I}_1 - \sigma_1\mathcal{I}_1, \\
{}^{\mathcal{RL}}\mathbf{D}^{\alpha}\mathcal{I}_2(\xi) &= \beta\xi^{\beta-1}G_3(\mathcal{S}, \mathcal{I}_1, \mathcal{I}_2, \mathcal{Q}, \mathcal{R}, \xi) = \beta_2\mathcal{I}_2\mathcal{S} + \delta_4\mathcal{Q} + \delta_1\mathcal{I}_1 - \gamma_2\mathcal{I}_2 - \delta_2\mathcal{I}_2 - \delta_3\mathcal{I}_2 - \mu\mathcal{I}_2 - \sigma_2\mathcal{I}_2, \\
{}^{\mathcal{RL}}\mathbf{D}^{\alpha}\mathcal{Q}(\xi) &= \beta\xi^{\beta-1}G_4(\mathcal{S}, \mathcal{I}_1, \mathcal{I}_2, \mathcal{Q}, \mathcal{R}, \xi) = \delta_3\mathcal{I}_2 - \gamma_3\mathcal{Q} - \delta_4\mathcal{Q} - \mu\mathcal{Q} - \sigma_3\mathcal{Q}, \\
{}^{\mathcal{RL}}\mathbf{D}^{\alpha}\mathcal{R}(\xi) &= \beta\xi^{\beta-1}G_5(\mathcal{S}, \mathcal{I}_1, \mathcal{I}_2, \mathcal{Q}, \mathcal{R}, \xi) = \sigma_1\mathcal{I}_1 + \sigma_2\mathcal{I}_2 + \sigma_3\mathcal{Q} - \mu\mathcal{R}.
\end{aligned}
\tag{3}
$$

The self-contained system (3) can be condensed into a compact framework as follows:

$$
\begin{cases}
{}^{\mathcal{RL}}\mathbf{D}^{\alpha}\Xi(\xi) = \beta\xi^{\beta-1}\chi(\xi, \Xi(\xi)), \ 0 < \alpha, \ \beta \leq 1, \\
\Xi(0) = \Xi_0.
\end{cases}
\tag{4}
$$

By substituting ${}^{\mathcal{RL}}\mathbf{D}^{\alpha,\beta}$ with ${}^{C}\mathbf{D}^{\alpha,\beta}$ and utilizing the Riemann-Liouville integral, the solution to Equation (4) will take on the following form:

$$
\Xi(\xi) = \Xi_0(\xi) + \frac{\beta}{\Gamma(\alpha)}\int_0^{\xi}(\xi - x)^{\alpha-1}x^{\beta-1}\chi(x, \Xi(x))dx,
\tag{5}
$$

where

$$
\Xi(\xi) = \begin{pmatrix} \mathcal{S}(\xi) \\ \mathcal{I}_1(\xi) \\ \mathcal{I}_2(\xi) \\ \mathcal{Q}(\xi) \\ \mathcal{R}(\xi) \end{pmatrix}, \quad \Xi_0(\xi) = \begin{pmatrix} \mathcal{S}_0 \\ \mathcal{I}_{10} \\ \mathcal{I}_{20} \\ \mathcal{Q}_0 \\ \mathcal{R}_0 \end{pmatrix}, \quad \chi(\xi, \Xi(\xi)) = \begin{pmatrix} \mathcal{G}_5(\mathcal{S}, \mathcal{I}_1, \mathcal{I}_2, \mathcal{Q}, \mathcal{R}, \xi) \\ \mathcal{G}_5(\mathcal{S}, \mathcal{I}_1, \mathcal{I}_2, \mathcal{Q}, \mathcal{R}, \xi) \\ \mathcal{G}_5(\mathcal{S}, \mathcal{I}_1, \mathcal{I}_2, \mathcal{Q}, \mathcal{R}, \xi) \\ \mathcal{G}_5(\mathcal{S}, \mathcal{I}_1, \mathcal{I}_2, \mathcal{Q}, \mathcal{R}, \xi) \\ \mathcal{G}_5(\mathcal{S}, \mathcal{I}_1, \mathcal{I}_2, \mathcal{Q}, \mathcal{R}, \xi) \end{pmatrix}.
$$

To transform system (1) into a fixed-point problem, we define the operator $\mathcal{P} : \mathbb{B} \to \mathbb{B}$ as follows:

$$
\mathcal{P}(\Xi)(\xi) = \Xi_0(\xi) + \frac{\beta}{\Gamma(\alpha)} \int_0^\xi x^{\beta-1}(\xi - x)^{\alpha-1} \chi(x, \Xi(x)) dx. \tag{6}
$$

5.1. Existence and Uniqueness Results

Using the theorems derived from the referenced source, we establish the existence results derived from the devised model [40].

Theorem 3. *A mapping that is completely continuous can be defined as $\mathcal{P} : \mathbb{B} \to \mathbb{B}$*

$$
\upsilon(\mathcal{P}) = \big\{ \Xi \in \mathbb{B} : \Xi = \zeta \mathcal{P}(\Xi), \ \zeta \in [0,1] \big\}.
$$

The boundedness of the operator $\mathcal{P}$ implies the existence of at least one fixed point in $\mathbb{B}$.

To verify the existence and stability analysis of the solution for the formulated model, we will examine the resulting propositions:

$(\mathcal{C})$For any Ξ and $\overline{\Xi}$ in $\mathcal{B}$, there exists a positive constant $\mathbb{M}_\chi$ such that the following condition holds:

$$
\big| \chi(\xi, \Xi) - \chi(\xi, \overline{\Xi}) \big| \leq \mathbb{M}_\chi |\Xi - \overline{\Xi}|.
$$

The representation described below can be utilized in several ways to achieve the desired results:

$$
\Delta = \frac{\beta \mathbb{P}^{\alpha+\beta-1} \mathbf{B}(\alpha, \beta)}{\Gamma(\alpha)}.
$$

In this scenario, the symbol $\mathbf{B}(\alpha, \beta)$ denotes the beta function.

Theorem 4. *If the operator χ, defined as $\chi : C[0,T] \times \mathbb{B} \to \mathbb{R}$, is continuous and condition $(\mathcal{C})$ can be satisfied, then there must be at least one solution to problem (2) for the system.*

Proof. Our initial objective is to show that the operator $\mathcal{P} : \mathbb{B} \to \mathbb{B}$ defined in (6) is completely continuous. Let's take a sequence Ξ_n such that Ξ_n converges to Ξ in $\mathbb{B}$, where $\xi \in [0,T]$. This sequence can be represented as:

$$
\begin{aligned}
\| \mathcal{P}(\Xi_n) - \mathcal{P}(\Xi) \| &\leq \frac{\beta}{\Gamma(\alpha)} \max_{\xi \in [0,T]} \int_0^\xi x^{\beta-1}(\xi-x)^{\alpha-1} |\chi(x, \Xi_n(x)) - \chi(x, \Xi(x))| dx, \\
&\leq \frac{\beta \mathcal{K}_\chi}{\Gamma(\alpha)} \| \Xi_n - \Xi \| \max_{\xi \in [0,T]} \int_0^\xi x^{\alpha-1}(1-x)^{\beta-1} \xi^{\alpha+\beta-1} dx, \\
&\leq \Delta \mathcal{K}_\chi \| \Xi_n - \Xi \|.
\end{aligned} \tag{7}
$$

Consequently, since Ξ_n converges to Ξ, it follows that $\| \mathcal{P}(\Xi_n) - \mathcal{P}(\Xi) \|$ tends to zero as n approaches zero. Therefore, the operator is continuous.

Suppose $\mathfrak{T}$ is a bounded set in $\mathbb{B}$. Then, there exists a constant $C_\chi > 0$ such that $|\chi(\xi, \Xi(\xi))| \leq C_\chi$ holds for all $\Xi \in \mathcal{B}$, and for any $\Xi \in \mathfrak{T}$, we can express this as:

$$
\begin{aligned}
\|\mathcal{P}(\Xi)\| &\leq \frac{\beta C_\chi}{\Gamma(\alpha)} \max_{\xi \in [0,T]} \left| \int_0^\xi (\xi - x)^{\alpha-1} x^{\beta-1} dx \right|, \\
&\leq \frac{\beta C_\chi}{\Gamma(\alpha)} \max_{\xi \in [0,T]} \int_0^\xi (1 - x)^{\beta-1} x^{\alpha-1} \xi^{\alpha+\beta-1} dx, \\
&\leq \Delta C_\chi.
\end{aligned}
\tag{8}
$$

Thus, Equation (8) signifies that the operator $\mathcal{P}$ is uniformly bounded.

Additionally, to confirm the equi-continuity of the operator $\mathcal{P}$, let's consider $0 \leq \xi_2 \leq \xi_1 \leq T$. We deduce the following outcome:

$$
\begin{aligned}
\|\mathcal{P}(\Xi(\xi_1)) - \mathcal{P}(\Xi(\xi_2))\| &\leq \frac{\beta C_\chi}{\Gamma(\alpha)} \max_{\xi \in [0,T]} \left| \int_0^{\xi_1} (\xi_1 - x)^{\alpha-1} x^{\beta-1} dx - \int_0^{\xi_2} (\xi_2 - x)^{\alpha-1} x^{\beta-1} dx \right|, \\
&\leq \frac{\beta C_\chi \mathbf{B}(\alpha, \beta)}{\Gamma(\alpha)} (\xi_1^{\alpha+\beta-1} - \xi_2^{\alpha+\beta-1}) \to 0 \ \text{as} \ \xi_1 \to \xi_2.
\end{aligned}
\tag{9}
$$

Hence, the operator $\mathcal{P}$ exhibits equi-continuity, boundedness, and continuity simultaneously. Therefore, by invoking the Arzela-Ascoli theorem, we can demonstrate that the operator $\mathcal{P}$ is relatively compact and completely continuous.

Consider the set v, defined as $v = \{\Xi \in \mathbb{B} : \Xi = \zeta, \mathcal{P}(\Xi), \zeta \in [0,1]\}$. Let's now confirm the boundedness of v. Take $\Xi \in v$; for $\xi \in [0,T]$, we find $\|\Xi\| = \Delta C_\chi$.

Thus, v is bounded. By Theorem (3), system (2) has at least one solution. □

We will utilize the fixed-point technique outlined in [40] to establish the uniqueness of the solution for model (2).

Theorem 5. *Given proposition $(\mathcal{C})$ and under the condition $\mathbf{H}_\chi \leq 1$, problem (2) can be uniquely resolved as follows:*

$$
\mathbf{H}_\chi = \Delta \mathbb{M}_\chi.
\tag{10}
$$

Proof. Let's define $\max_{\xi \in [0,T]} |\chi(\xi, 0)| = \mathcal{K}_\chi < \infty$, such that $\varrho \geq \frac{\Delta \mathcal{K}_\chi}{1 - \Delta \mathbb{M}_\chi}$. Our objective is to prove that $\mathcal{P}(\mathcal{B}\varrho) \subset \mathcal{B}\varrho$, where $\mathcal{B}\varrho = \{\Xi \in \mathbb{B} : \|\Xi\| \leq \varrho\}$ and $\Xi \in \mathcal{B}_\varrho$. We have:

$$
\begin{aligned}
\|\mathcal{P}(\Xi)\| &\leq \frac{\beta}{\Gamma(\alpha)} \max_{\xi \in [0,T]} \int_0^\xi (\xi - x)^{\alpha-1} x^{\beta-1} \bigg(|\chi(\xi, \Xi(\xi)) - \chi(\xi, 0)| + |\chi(\xi, 0)| \bigg) dx, \\
&\leq \frac{\beta \mathbb{P}^{\alpha+\beta-1} \mathbf{B}(\alpha, \beta)(\mathbb{M}_\chi \|\Xi\| + \mathcal{K}_\chi)}{\Gamma(\alpha)}, \\
&\leq \Delta(\mathbb{M}_\chi \varrho + \mathcal{K}_\chi), \\
&\leq \varrho.
\end{aligned}
\tag{11}
$$

The operator $\mathcal{P} : \mathbb{B} \to \mathbb{B}$ described in (6) is subject to proposition $(\mathcal{C})$, which asserts the following condition for all $\xi \in [0,T]$, Ξ, and $\overline{\Xi} \in \mathbb{B}$:

$$
\begin{aligned}
\|\mathcal{P}(\Xi) - \mathcal{P}(\overline{\Xi})\| &\leq \frac{\beta}{\Gamma(\alpha)} \max_{\xi \in [0,T]} \left| \int_0^\xi (\xi - x)^{\alpha-1} x^{\beta-1} \chi(x, \Xi(x)) dx - \int_0^\xi (\xi - x)^{\alpha-1} x^{\beta-1} \chi(x, \overline{\Xi}(x)) dx \right|, \\
&\leq \mathbf{H}_\chi \|\Xi - \overline{\Xi}\|.
\end{aligned}
\tag{12}
$$

Thus, due to the contraction property of the operator $\mathcal{P}$, the formulated model (2) has a unique solution. □

5.2. Ulam-Hyers Stability Analysis

This section is dedicated to conducting Ulam-Hyers (UH) stability analysis to confirm the stability of the formulated model (2).

Definition 5. *For the formulated model to be considered Ulam-Hyers (UH) stable, it must satisfy a condition where there exists a $\Re_{\alpha,\beta} > 0$ such that for any $\rho > 0$ and every $\Xi \in C([0,T],\mathbb{R})$, the subsequent condition holds:*

$$\left| {}^{\mathcal{FF}}\mathbf{D}_\xi^{\alpha,\,\beta}\Xi(\xi) - \chi(\xi,\Xi(\xi)) \right| \leq \rho, \ \xi \in [0,T], \tag{13}$$

and there exists a unique solution $\Phi \in C([0,T],\mathbb{R})$ such that

$$\left| \Xi(\xi) - \Phi(\xi) \right| \leq \Re_{\alpha,\beta}\rho, \ \xi \in [0,T]. \tag{14}$$

Suppose there exists a small perturbation $\chi \in C([0,T],\mathbb{R})$ such that $\chi(0) = 0$. We will observe:

- $|\chi(\xi)| \leq \rho$, for $\rho > 0$;

- ${}^{\mathcal{FF}}\mathbf{D}_\xi^{\alpha,\,\beta}\Xi(\xi) = \chi(\xi,\Xi(\xi)) + \chi(\xi)$.

Lemma 3. *The solution to the perturbed equation*

$$\begin{aligned} {}^{\mathcal{FF}}\mathbf{D}_\xi^{\alpha,\,\beta}\Xi(\xi) &= \chi(\xi,\Xi(\xi)) + \chi(\xi), \\ \Xi(0) &= \Xi_0, \end{aligned} \tag{15}$$

fulfills the following relation:

$$\left| \Xi(\xi) - \left(\Xi_0(\xi) + \frac{\beta}{\Gamma(\alpha)} \int_0^\xi x^{\beta-1}(\xi-x)^{\alpha-1}\chi(x,\Xi(x))dx \right) \right| \leq \mathbb{C}_{\alpha,\,\beta}\,\rho, \tag{16}$$

where $\left(\frac{\beta}{\Gamma(\alpha)}\mathbb{P}^{\alpha+\beta-1}\mathbf{B}(\alpha,\beta) \right) = \mathbb{C}_{\alpha,\,\beta}\,\rho$.

Proof. For simplicity, we will refrain from delving into the proof. □

Theorem 6. *Given Proposition $(\mathcal{C})$ and Lemma 3, the solution to integral Equation (2) is deemed Ulam-Hyers stable, provided that the condition $\mathbf{H}_\chi < 1$ is satisfied.*

Proof. Let $Z \in \mathbb{B}$ denote the unique solution to the proposed model, and consider $\Xi \in \mathbb{B}$ as any solution that satisfies Equation (5). By employing fractal-fractional integration, we derive the following expression:

$$\begin{aligned} |\Xi(\xi) - Z(\xi)| &= \left| \Xi(\xi) - \left(Z_0(\xi) + \frac{\beta}{\Gamma(\alpha)} \int_0^\xi (\xi-x)^{\alpha-1}x^{\beta-1}\chi(x,Z(x))dx \right) \right|, \\ &\leq \left| \Xi(\xi) - \left(\Xi_0(\xi) + \frac{\beta}{\Gamma(\alpha)} \int_0^\xi (\xi-x)^{\alpha-1}x^{\beta-1}\chi(x,\Xi(x))dx \right) \right| \\ &\quad + \left| \left(\Xi_0(\xi) + \frac{\beta}{\Gamma(\alpha)} \int_0^\xi (\xi-x)^{\alpha-1}x^{\beta-1}\chi(x,\Xi(x))dx \right) - \left(Z_0(\xi) + \frac{\beta}{\Gamma(\alpha)} \int_0^\xi (\xi-x)^{\alpha-1}x^{\beta-1}\chi(x,Z(x))dx \right) \right|, \\ &\leq \mathbb{C}_{\alpha,\beta}\,\rho + \frac{\beta}{\Gamma(\alpha)}\mathbb{P}^{\alpha+\beta-1}\mathbb{M}_\chi\mathbf{B}(\alpha,\beta)\|\Xi(\xi) - Z(\xi)\|, \\ &\leq \mathbb{C}_{\alpha,\,\beta}\rho + \mathbf{H}_\chi\|\Xi(\xi) - Z(\xi)\|. \end{aligned} \tag{17}$$

Hence, we can state:

$$\|\Xi - Z\| \leq \mathbb{C}_{\alpha,\,\beta}\rho + \mathbf{H}_\chi\|\Xi - Z\|. \tag{18}$$

The Equation (18) can be expressed as follows:

$$\|\Xi - Z\| \leq \Re_{\alpha,\,\beta}\,\rho. \tag{19}$$

Therefore, $\Re_{\alpha,\beta} = \left(\dfrac{\mathbb{C}\alpha,\beta}{1-\mathbf{H}\chi}\right)$. This indicates that the solution to Equation (5) demonstrates UH stability, thus confirming the Ulam-Hyers stability of the solution to the proposed model (2). $\square$

6. Numerical Method for Fractal-Fractional Model

In this section, our goal is to delineate a numerical method for simulating the formulated model using computational techniques. To achieve this, we will employ the Caputo derivative and its corresponding integral to convert the model (5) into the following format:

$$
\begin{aligned}
\mathcal{S}(\xi) &= \mathcal{S}(0) + \frac{\beta}{\Gamma(\alpha)} \int_0^{\xi} x^{\beta-1}(\xi - x)^{\alpha-1}\mathcal{G}_1(\mathcal{S},\mathcal{I}_1,\mathcal{I}_2,\mathcal{Q},\mathcal{R},x)dx, \\[2mm]
\mathcal{I}_1(\xi) &= \mathcal{I}_1(0) + \frac{\beta}{\Gamma(\alpha)} \int_0^{\xi} x^{\beta-1}(\xi - x)^{\alpha-1}\mathcal{G}_2(\mathcal{S},\mathcal{I}_1,\mathcal{I}_2,\mathcal{Q},\mathcal{R},x)dx, \\[2mm]
\mathcal{I}_2(\xi) &= \mathcal{I}_2(0) + \frac{\beta}{\Gamma(\alpha)} \int_0^{\xi} x^{\beta-1}(\xi - x)^{\alpha-1}\mathcal{G}_3(\mathcal{S},\mathcal{I}_1,\mathcal{I}_2,\mathcal{Q},\mathcal{R},x)dx, \\[2mm]
\mathcal{Q}(\xi) &= \mathcal{Q}(0) + \frac{\beta}{\Gamma(\alpha)} \int_0^{\xi} x^{\beta-1}(\xi - x)^{\alpha-1}\mathcal{G}_4(\mathcal{S},\mathcal{I}_1,\mathcal{I}_2,\mathcal{Q},\mathcal{R},x)dx, \\[2mm]
\mathcal{R}(\xi) &= \mathcal{R}(0) + \frac{\beta}{\Gamma(\alpha)} \int_0^{\xi} x^{\beta-1}(\xi - x)^{\alpha-1}\mathcal{G}_5(\mathcal{S},\mathcal{I}_1,\mathcal{I}_2,\mathcal{Q},\mathcal{R},x)dx.
\end{aligned} \tag{20}
$$

Next, we will demonstrate the numerical solution of Equation (20) at discrete-time instances $\xi = \xi_{m+1}$ for $m = 0, 1, 2, \ldots$ using the new approach. This enables us to illustrate the first equation of the system outlined above.

$$\mathcal{S}_{m+1}(\xi) = \mathcal{S}(0) + \frac{\beta}{\Gamma(\alpha)} \int_0^{\xi_{m+1}} x^{\beta-1}(\xi_{m+1} - x)^{\alpha-1}\mathcal{G}_1(\mathcal{S},\mathcal{I}_1,\mathcal{I}_2,\mathcal{Q},\mathcal{R},x)\,dx, \tag{21}$$

and

$$\mathcal{S}_m(\xi) = \mathcal{S}(0) + \frac{\beta}{\Gamma(\alpha)} \int_0^{\xi_m} x^{\beta-1}(\xi_m - x)^{\alpha-1}\mathcal{G}_1(\mathcal{S},\mathcal{I}_1,\mathcal{I}_2,\mathcal{Q},\mathcal{R},x)\,dx. \tag{22}$$

Additionally, it's important to note that the approximate integral form obtained from the equation above can be succinctly summarized as follows:

$$\mathcal{S}_{m+1}(\xi) = \mathcal{S}(0) + \frac{\beta}{\Gamma(\alpha)} \sum_{i=0}^{m} \int_{\xi_i}^{\xi_{i+1}} x^{\beta-1}(\xi_{m+1} - x)^{\alpha-1}\mathcal{G}_1(\mathcal{S},\mathcal{I}_1,\mathcal{I}_2,\mathcal{Q},\mathcal{R},x)\,dx. \tag{23}$$

In the infinite interval $[\xi_i, \xi_{i+1}]$, the function $\mathcal{G}_1(\mathcal{S},\mathcal{I}_1,\mathcal{I}_2,\mathcal{Q},\mathcal{R},x)$ approximates the step size of the interpolation by employing Lagrange interpolation with $h = [\xi_i - \xi_{i-1}]$. This is expressed as:

$$\mathcal{S}_m^*(\xi) \approx \frac{1}{h}\left[(\xi - \xi_{i-1})\xi_i^{\beta-1}\mathcal{G}_1(\mathcal{S}_i,\mathcal{I}_{1(i)},\mathcal{I}_{2(i)},\mathcal{Q}_i,\mathcal{R}_i,\xi_i) - (\xi - \xi_i)\xi_{i-1}^{\beta-1}\mathcal{G}_1(\mathcal{S}_{i-1},\mathcal{I}_{1(i-1)},\mathcal{I}_{2(i-1)},\mathcal{Q}_{i-1},\mathcal{R}_{i-1},\xi_{i-1})\right]. \tag{24}$$

Replacing Equation (24) with Equation (23) results in the following expression:

$$\mathcal{S}_{m+1}(\xi) = \mathcal{S}(0) + \frac{\beta}{\Gamma(\alpha)} \sum_{i=0}^{m} \int_{\xi_i}^{\xi_{i+1}} x^{\beta-1}(\xi_{m+1} - x)^{\alpha-1}\mathcal{G}_1(\mathcal{S},\mathcal{I}_1,\mathcal{I}_2,\mathcal{Q},\mathcal{R},x)\,\mathcal{S}_m^*(\xi)\,dx. \tag{25}$$

The numerical iterative solution for the $\mathcal{S}$ class of the formulated model using the Caputo operator with fractal-fractional derivative requires evaluating the integral on the right-hand side of Equation (25) as follows:

$$
\mathcal{S}_{m+1} =
\begin{cases}
\mathcal{S}_0 + \frac{\beta h^\alpha}{\Gamma(\alpha+2)} \sum\limits_{i=0}^{m} \left[(\xi_i^{\beta-1}) \mathcal{G}_1(\mathcal{S}_i, \mathcal{I}_{1(i)}, \mathcal{I}_{2(i)}, \mathcal{Q}_i, \mathcal{R}_i, \xi_i) \times \left((m+1-i)^\beta (m-i+2+\beta) - (m-i)^\beta (m-i+2+2\beta) \right) \right. \\
\left. - \xi_{i-1}^{\beta-1} \mathcal{G}_1(\mathcal{S}_{i-1}, \mathcal{I}_{1(i-1)}, \mathcal{I}_{2(i-1)}, \mathcal{Q}_{i-1}, \mathcal{R}_{i-1}, \xi_{i-1}) \times \left((m+1-i)^\beta + 1 - (m-i)^\beta (m-i+1+\beta) \right) \right].
\end{cases}
\tag{26}
$$

Consequently, the remaining terms in the formulated model concerning the respective compartments can be articulated as follows:

$$
\mathcal{I}_{1(m+1)} =
\begin{cases}
\mathcal{I}_1(0) + \frac{\beta h^\alpha}{\Gamma(\alpha+2)} \sum\limits_{i=0}^{m} \left[(\xi_i^{\beta-1}) \mathcal{G}_2(\mathcal{S}_i, \mathcal{I}_{1(i)}, \mathcal{I}_{2(i)}, \mathcal{Q}_i, \mathcal{R}_i, \xi_i) \times \left((m+1-i)^\beta (m-i+2+\beta) - (m-i)^\beta (m-i+2+2\beta) \right) \right. \\
\left. - \xi_{i-1}^{\beta-1} \mathcal{G}_2(\mathcal{S}_{i-1}, \mathcal{I}_{1(i-1)}, \mathcal{I}_{2(i-1)}, \mathcal{Q}_{i-1}, \mathcal{R}_{i-1}, \xi_{i-1}) \times \left((m+1-i)^\beta + 1 - (m-i)^\beta (m-i+1+\beta) \right) \right].
\end{cases}
\tag{27}
$$

$$
\mathcal{I}_{2(m+1)} =
\begin{cases}
\mathcal{I}_2(0) + \frac{\beta h^\alpha}{\Gamma(\alpha+2)} \sum\limits_{i=0}^{m} \left[(\xi_i^{\beta-1}) \mathcal{G}_3(\mathcal{S}_i, \mathcal{I}_{1(i)}, \mathcal{I}_{2(i)}, \mathcal{Q}_i, \mathcal{R}_i, \xi_i) \times \left((m+1-i)^\beta (m-i+2+\beta) - (m-i)^\beta (m-i+2+2\beta) \right) \right. \\
\left. - \xi_{i-1}^{\beta-1} \mathcal{G}_3(\mathcal{S}_{i-1}, \mathcal{I}_{1(i-1)}, \mathcal{I}_{2(i-1)}, \mathcal{Q}_{i-1}, \mathcal{R}_{i-1}, \xi_{i-1}) \times \left((m+1-i)^\beta + 1 - (m-i)^\beta (m-i+1+\beta) \right) \right].
\end{cases}
\tag{28}
$$

$$
\mathcal{Q}_{m+1} =
\begin{cases}
\mathcal{Q}_0 + \frac{\beta h^\alpha}{\Gamma(\alpha+2)} \sum\limits_{i=0}^{m} \left[(\xi_i^{\beta-1}) \mathcal{G}_4(\mathcal{S}_i, \mathcal{I}_{1(i)}, \mathcal{I}_{2(i)}, \mathcal{Q}_i, \mathcal{R}_i, \xi_i) \times \left((m+1-i)^\beta (m-i+2+\beta) - (m-i)^\beta (m-i+2+2\beta) \right) \right. \\
\left. - \xi_{i-1}^{\beta-1} \mathcal{G}_4(\mathcal{S}_{i-1}, \mathcal{I}_{1(i-1)}, \mathcal{I}_{2(i-1)}, \mathcal{Q}_{i-1}, \mathcal{R}_{i-1}, \xi_{i-1}) \times \left((m+1-i)^\beta + 1 - (m-i)^\beta (m-i+1+\beta) \right) \right].
\end{cases}
\tag{29}
$$

$$
\mathcal{R}_{m+1} =
\begin{cases}
\mathcal{R}_0 + \frac{\beta h^\alpha}{\Gamma(\alpha+2)} \sum\limits_{i=0}^{m} \left[(\xi_i^{\beta-1}) \mathcal{G}_5(\mathcal{S}_i, \mathcal{I}_{1(i)}, \mathcal{I}_{2(i)}, \mathcal{Q}_i, \mathcal{R}_i, \xi_i) \times \left((m+1-i)^\beta (m-i+2+\beta) - (m-i)^\beta (m-i+2+2\beta) \right) \right. \\
\left. - \xi_{i-1}^{\beta-1} \mathcal{G}_5(\mathcal{S}_{i-1}, \mathcal{I}_{1(i-1)}, \mathcal{I}_{2(i-1)}, \mathcal{Q}_{i-1}, \mathcal{R}_{i-1}, \xi_{i-1}) \times \left((m+1-i)^\beta + 1 - (m-i)^\beta (m-i+1+\beta) \right) \right].
\end{cases}
\tag{30}
$$

Numerical Experimentation and Discussion

In this section, we delve into the numerical simulation of our proposed scheme using a fractal-fractional approach to model HIV disease dynamics. We emphasize the intricate relationships among model parameters and their combined impact on HIV transmission across three infection levels within the community. Our HIV fractional-order model is designed to analyze disease transmission through simulations, employing fractal-fractional derivatives with a power-law representation. The initial compartmental conditions, as detailed in [2], are set as follows: $\mathcal{S}(0) = 5726$, $\mathcal{I}_1(0) = 70$, $\mathcal{I}_2(0) = 40$, $\mathcal{Q}(0) = 10$, and $\mathcal{R}(0) = 0$. Fractional values are instrumental in discerning outcomes within this nonlinear system. To ensure the study's robustness, we adopt parameter values from Table 1 based on established literature. Our model yields compelling results by incorporating non-integer parameter values. Adjusting fractional values with precision enables us to derive solutions for variables $\mathcal{S}$, $\mathcal{I}_1$, $\mathcal{I}_2$, $\mathcal{Q}$, and $\mathcal{R}$, as depicted in Figures 1–5. We utilize MATLAB for numerical simulations spanning 500 days with a time step of $h = 0.03$. Our exploration encompasses five distinct cases where we vary the fractional orders (α) and dimensions (β) of the independent variable ξ, aiming to deepen our understanding of the model's behavior.

Moreover, by employing the fractal-fractional derivative with the Caputo operator, our model generates numerical outputs for various fractional values, focusing on the steady-state point. The graphical representation of the HIV transmission model using our proposed numerical method and the comparison between fractal-fractional and integer orders are illustrated in Figures 1–5. All trajectories demonstrate a consistent pattern, converging to the true endemic equilibrium point. Initially, we maintain a proportional relationship between the fractal order (α) and fractional dimension (β) of the independent variable ξ, ensuring $\alpha = \beta$. We then explore variations in these values, setting $\alpha = 0.80, 0.85, 0.90, 0.95, 1.00$ and $\beta = 0.80, 0.85, 0.90, 0.95, 1.00$, over a time span of $\xi \in [0, 500]$ units (days) with a time step

of $h = 0.03$. This exploration elucidates the impact of different fractal orders and dimensions on the trajectories of compartmental classes in the HIV transmission model. Each combination of α and β unveils distinct patterns and behaviors, as depicted in Figure 1a–e. Each trajectory, corresponding to a specific fractional order α and fractal dimension β, represents the disease dynamics within the modeled population. Notably, each graph exhibits varying rates of convergence based on fractal order and dimension, while all converge to a steady state.

Table 1. Parameters and its values.

Parameters	Values	Source	Parameters	Values	Source
Λ	$200.88\,\text{day}^{-1}$	[43]	β_1	$0.0000405\,\text{day}^{-1}$	[44]
β_2	$0.0000483\,\text{day}^{-1}$	[44]	γ_1	$0.01\,\text{day}^{-1}$	[45]
γ_2	$0.02\,\text{day}^{-1}$	[45]	γ_3	$0.04\,\text{day}^{-1}$	[46]
δ_1	$9.2274 \times 10^{-3}\,\text{day}^{-1}$	[47] and estimate	δ_2	$8.0037 \times 10^{-3}\,\text{day}^{-1}$	[47] and estimate
δ_3	$2.8595 \times 10^{-3}\,\text{day}^{-1}$	[47] and estimate	δ_4	$1.8595 \times 10^{-3}\,\text{day}^{-1}$	[47] and estimate
σ_1	$0.1\,\text{day}^{-1}$	[2] and estimate	σ_2	$0.2\,\text{day}^{-1}$	[2] and estimate
σ_3	$0.2\,\text{day}^{-1}$	[2] and estimate	μ	$0.01\,\text{day}^{-1}$	[45]

Figure 1a illustrates the evolution of the susceptible class $\mathcal{S}$ over time, considering constant fractional orders and dimensions. Different fractional orders exhibit varying slopes, impacting the dynamics of susceptibility in HIV transmission. Initially, the susceptible population experiences a rapid reduction at lower fractional orders but stabilizes to a steady state over time. This demonstrates how varying levels of memory and complexity influence the rate of change in susceptibility over time. Fractal dimensions remain stable, indicating a consistent transmission pattern, while varying slopes for the same fractional orders highlight the nuanced effects of memory. The initial decline followed by stabilization reflects a balance between exposure and immunity, akin to real-world scenarios where populations reach a stable risk level due to HIV exposure. Higher fractional orders suggest a more intricate interplay of factors affecting susceptibility, implying a more efficient utilization of historical data or long-term memory in the transmission process.

In Figure 1b, we present the dynamic behavior of the infective population at stage 1, denoted as $\mathcal{I}_1(\xi)$. The infected population demonstrates rapid growth as the fractional order α increases. Subsequently, decreasing the fractional order leads to a decline in the infected population. This trend stabilizes over time, indicating a more established state of infection within the population. The initial rapid increase followed by a gradual decrease in the infective population mirrors the dynamic nature of HIV transmission, as observed in real-world scenarios. This pattern reflects the early surge in infections as the virus spreads, followed by a period during which interventions, immunity, or other factors contribute to a reduction in new infections. Figure 1c illustrates the dynamics of the HIV-infected population at stage 2, denoted as $\mathcal{I}_2(\xi)$. The initial increase in the infected population is observed for higher fractional orders, followed by a decrease for lower fractional orders. These dynamics are influenced by various factors, including intervention strategies, transmission rates, and the interaction between different stages of infection.

Figure 1d illustrates the dynamic behavior of populations undergoing treatment, denoted as $\mathcal{Q}(\xi)$. This figure illustrates an increasing number of individuals recovering from HIV infection, reflecting the dynamic response of infective populations to treatment interventions. The decline in infected individuals is gradual as fractional orders increase, highlighting the sensitivity of dynamics to different parameter settings. Such dynamics mirror real-world scenarios where treatment plays a critical role in reducing infection rates and improving outcomes for individuals affected by HIV.

On the other hand, Figure 1e delves into the behavior of the recovered population, $\mathcal{R}(\xi)$. It depicts how HIV-recovered populations engage in treatment-seeking behavior, initially surging and then gradually declining. Notably, the recovered population increases

quickly with lower fractional orders, with the decline being more pronounced for higher fractional orders. These findings underscore the significant influence of fractional orders and fractal dimensions on HIV transmission dynamics and treatment decisions, providing valuable insights into the complex interplay between these parameters and HIV dynamics.
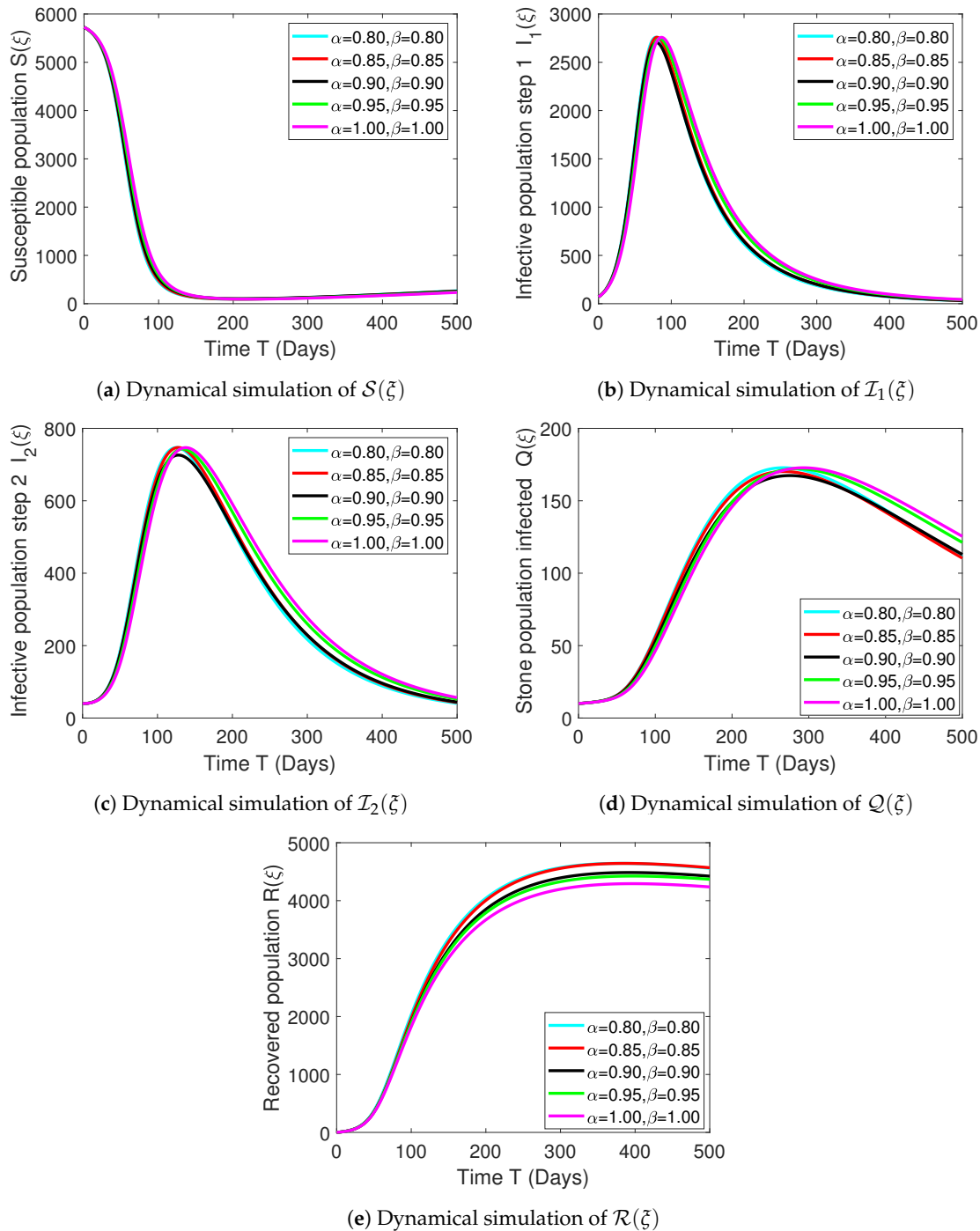

(**a**) Dynamical simulation of $\mathcal{S}(\xi)$

(**b**) Dynamical simulation of $\mathcal{I}_1(\xi)$

(**c**) Dynamical simulation of $\mathcal{I}_2(\xi)$

(**d**) Dynamical simulation of $\mathcal{Q}(\xi)$

(**e**) Dynamical simulation of $\mathcal{R}(\xi)$

Figure 1. The numerical simulation results show the behaviors of all compartments in the devised model under uniform fractional orders and fractal dimensions, specifically when $\alpha = \beta$.

In the second case, the analysis focuses solely on the fractional order α while keeping the fractal dimension β fixed at $\beta = 1$. The study examines a range of α values, specifically ($\alpha = 0.80, 0.85, 0.90, 0.95$, and 1.00), to explore how variations in fractional orders impact the dynamics of the HIV model across different infection levels, recovery stages, and treatment decisions. Figure 2a–e depict each trajectory against a specific value of fractional order α at

fractal dimension $\beta = 1$, illustrating the disease dynamics of the HIV model population. It is evident that each graph exhibits a different rate of convergence (based on fractional order α), but each curve ultimately reaches a steady state.

(**a**) Dynamical simulation of $\mathcal{S}(\xi)$

(**b**) Dynamical simulation of $\mathcal{I}_1(\xi)$

(**c**) Dynamical simulation of $\mathcal{I}_2(\xi)$

(**d**) Dynamical simulation of $\mathcal{Q}(\xi)$
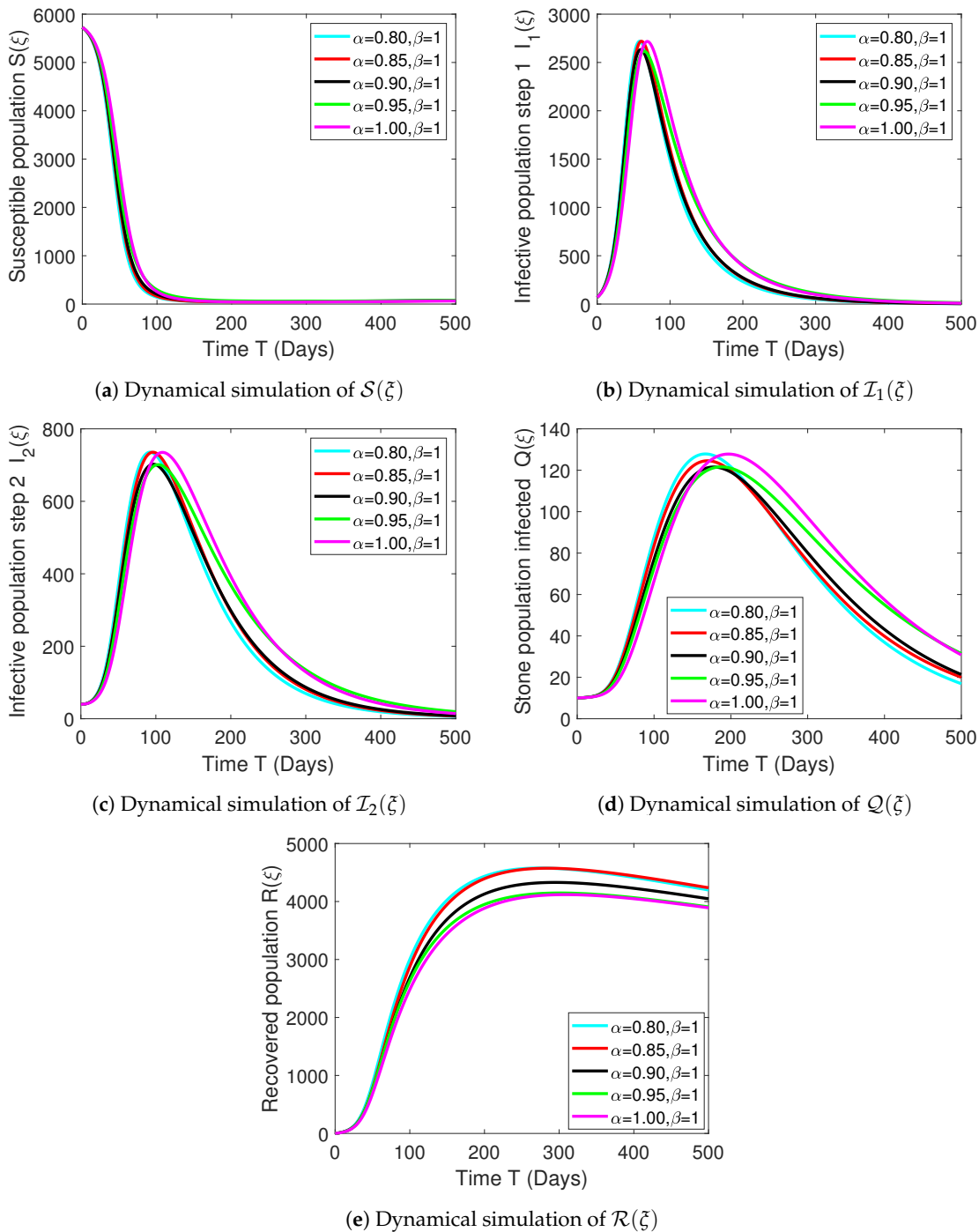

(**e**) Dynamical simulation of $\mathcal{R}(\xi)$

Figure 2. The numerical simulations illustrate the behaviors of all compartments in the devised model, specifically by varying the fractional order α while keeping β constant at a value of 1.

In the third exploration case, the model dynamics are analyzed by varying the fractal dimension ($\beta = 0.80, 0.85, 0.90, 0.95$, and 1.00), while keeping the fractional order fixed at $\alpha = 1$. By examining the impact of changing fractal dimensions on HIV transmission dynamics, the study aims to isolate the effects of β while holding α constant. Results depicted in Figure 3a–e illustrate how altering β influences the number of HIV cases across different compartments of the model ($\mathcal{S}, \mathcal{I}_1, \mathcal{I}_2, \mathcal{Q}$, and $\mathcal{R}$), providing insights into

the intricate dynamics of HIV spread. The curves resulting from fractional differential equations (2) clearly demonstrate a notably slower rise or decay over prolonged periods compared to those derived from a classical model with $\alpha = 1$. Across all figures, the dynamics tend toward a stable state as the fractional order decreases from 1 to 0.80 or lower. This indicates that a smaller fractional value leads to a more effective solution.
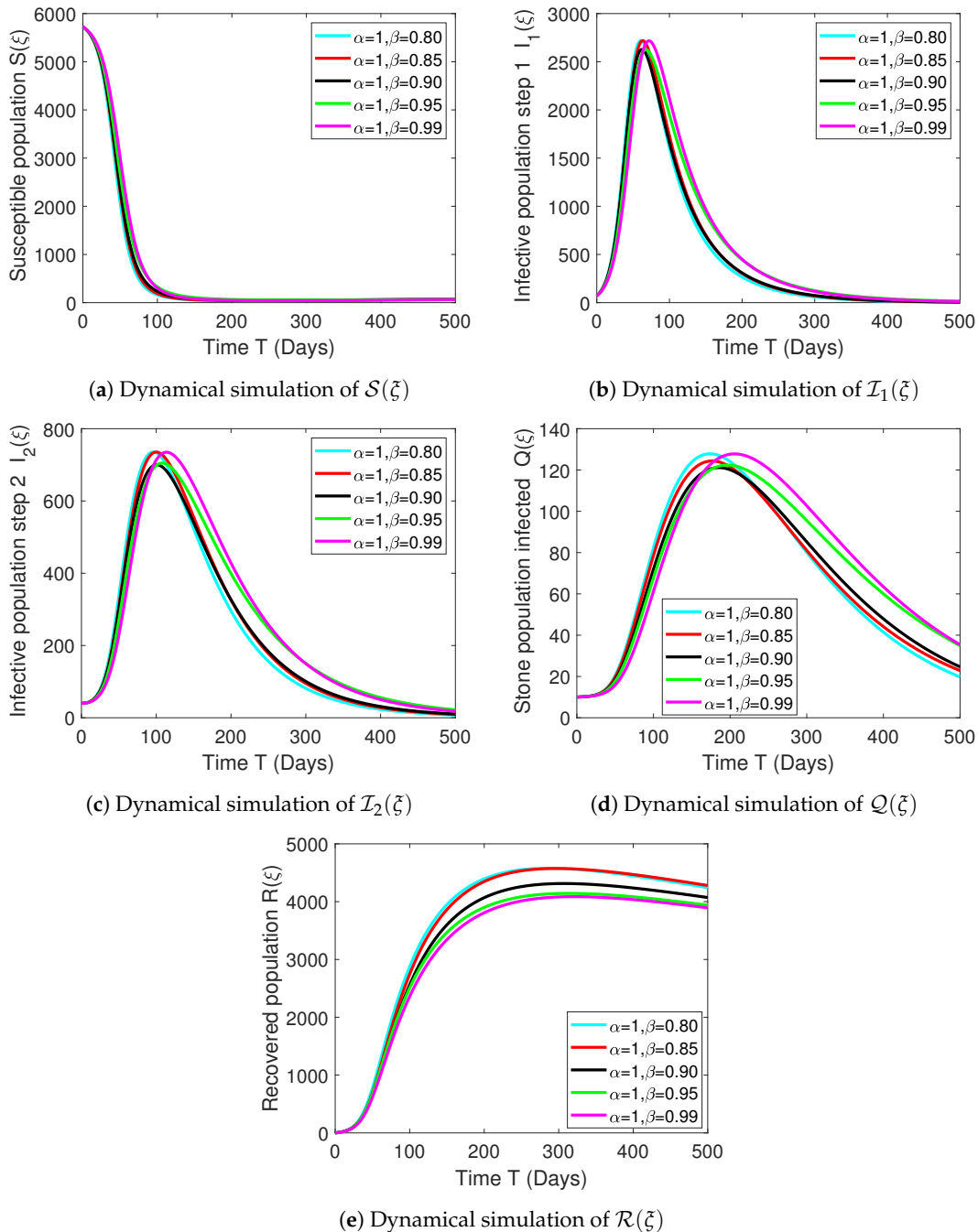

(**a**) Dynamical simulation of $\mathcal{S}(\xi)$

(**b**) Dynamical simulation of $\mathcal{I}_1(\xi)$

(**c**) Dynamical simulation of $\mathcal{I}_2(\xi)$

(**d**) Dynamical simulation of $\mathcal{Q}(\xi)$

(**e**) Dynamical simulation of $\mathcal{R}(\xi)$

Figure 3. The numerical simulations showcase the behaviors of all compartments in the devised model by varying the fractal dimensions while keeping the fractional order α fixed at 1.

In Figure 4a–e, we plot approximate solutions against different fractional orders at a fractional dimension of $\beta = 0.7$, covering fractional orders of $\alpha = 0.80, 0.85, 0.90, 0.95$, and 1.00. In Figure 5a–e, we investigate model dynamics by varying the fractional order ($\beta = 0.80, 0.85, 0.90, 0.95$, and 1.00) while maintaining a constant fractal dimension of $\beta = 0.9$. This case uniquely explores the influence of changing fractional orders on HIV model dynamics, impacting the reduction in deaths and HIV transmission. Additionally, we

derive significant insights from the model's compartments ($\mathcal{S}$, $\mathcal{I}_1$, $\mathcal{I}_2$, $\mathcal{Q}$, and $\mathcal{R}$), revealing the intricate dynamics of HIV spread. Observing Figures 4 and 5, we note that at a large value of fractal dimension, the graphs tend to reach a steady state more rapidly compared to a small value.
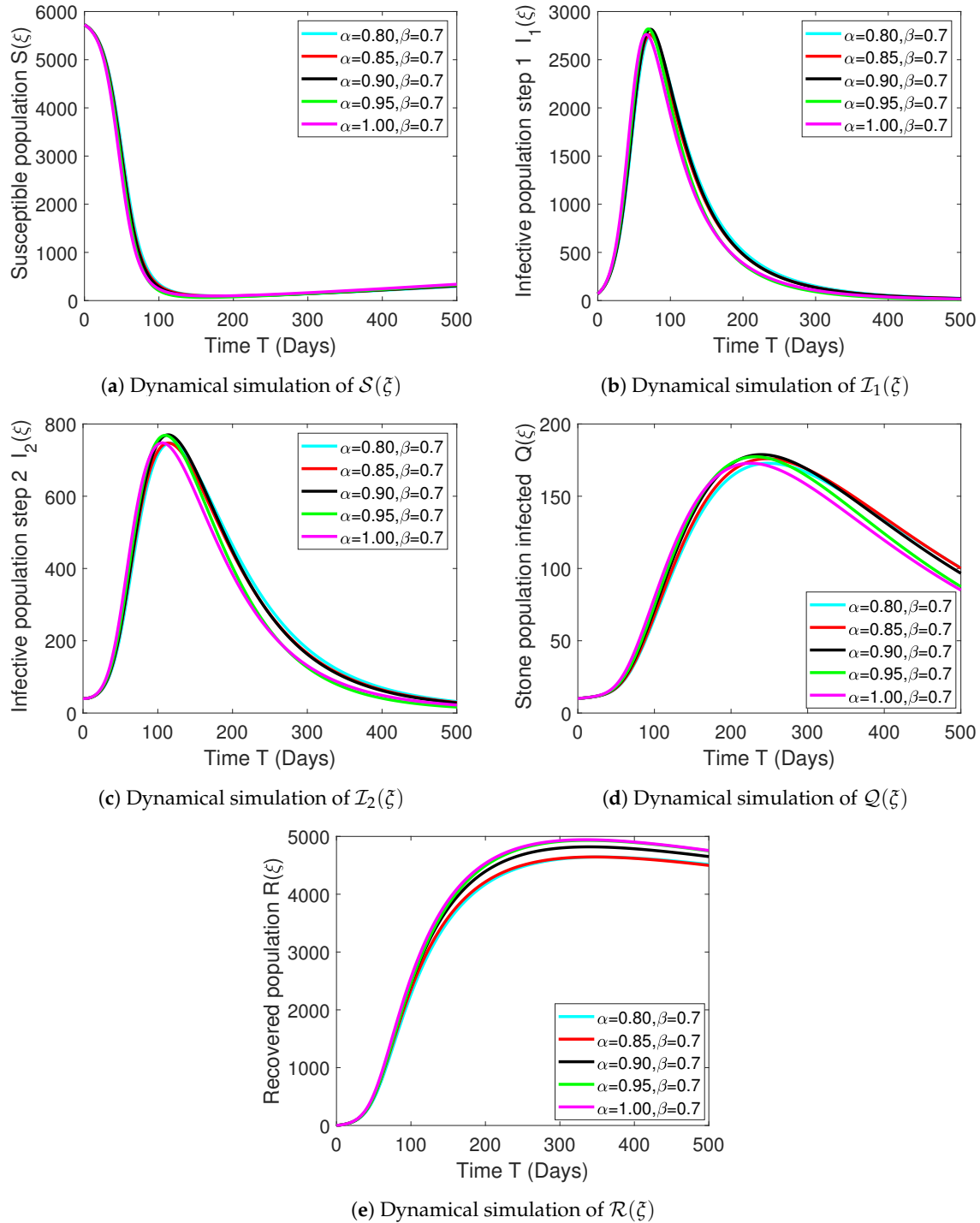

(**a**) Dynamical simulation of $\mathcal{S}(\xi)$

(**b**) Dynamical simulation of $\mathcal{I}_1(\xi)$

(**c**) Dynamical simulation of $\mathcal{I}_2(\xi)$

(**d**) Dynamical simulation of $\mathcal{Q}(\xi)$

(**e**) Dynamical simulation of $\mathcal{R}(\xi)$

Figure 4. The numerical simulations display how the compartments in the model respond over time, varying the fractional order α while maintaining a fixed dimension $\beta = 0.7$.
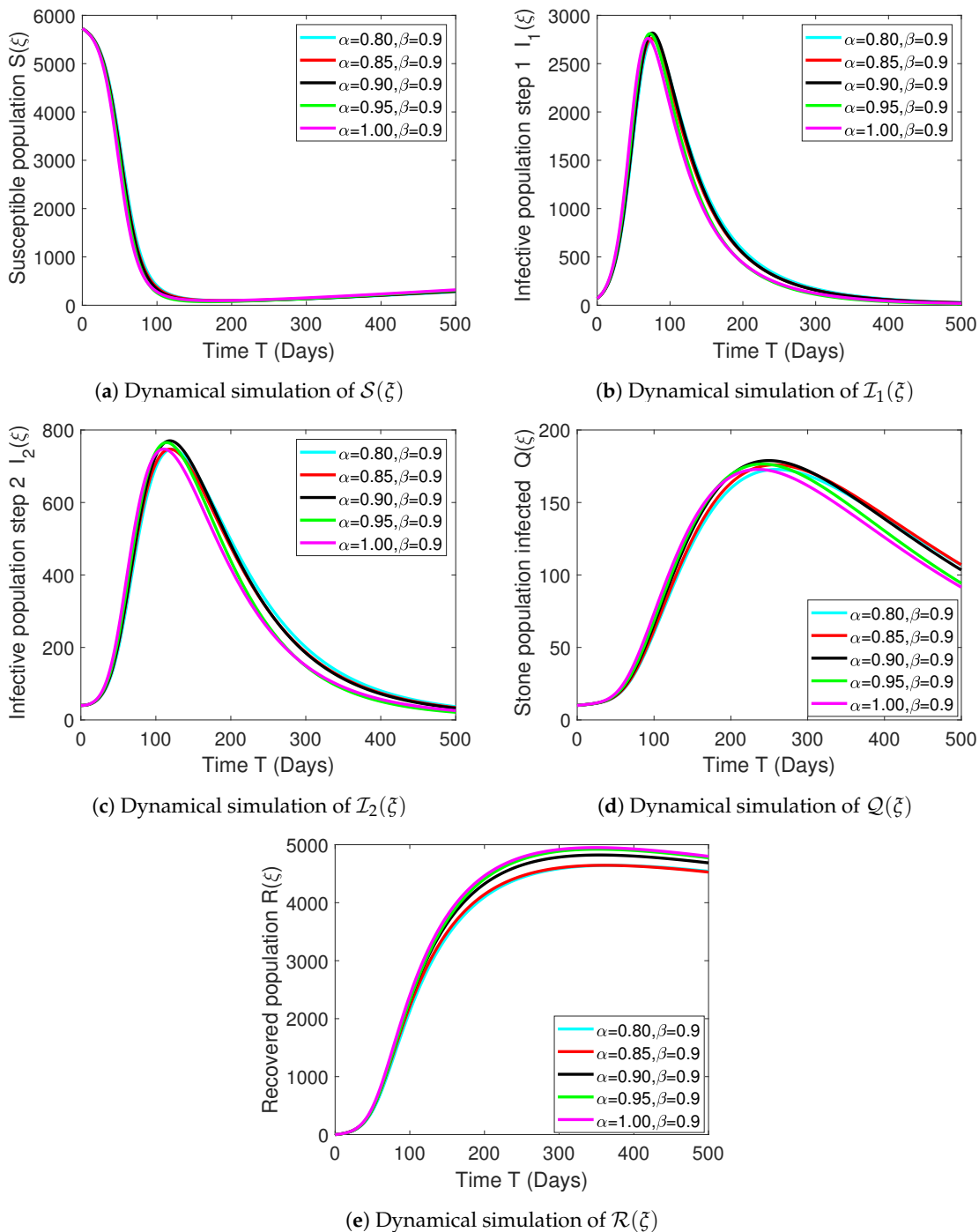
(**a**) Dynamical simulation of $\mathcal{S}(\xi)$

(**b**) Dynamical simulation of $\mathcal{I}_1(\xi)$

(**c**) Dynamical simulation of $\mathcal{I}_2(\xi)$

(**d**) Dynamical simulation of $\mathcal{Q}(\xi)$

(**e**) Dynamical simulation of $\mathcal{R}(\xi)$

Figure 5. The simulations show how the model's compartments respond over time, changing the fractional order α while holding the dimension $\beta = 0.9$ constant.

The newly generated fractal-fractional derivative model with the power-law kernel allows for the consideration of anomalous spread, similar to infection biological models. This new model avoids the inclusion of artificial singularities seen in the Riemann-Liouville-Caputo case, providing a more accurate description of the biological process's history. Non-local operators, a powerful mathematical tool for describing non-local phenomena following the power-law, have been utilized in this context. Numerical simulations depicted in the figures show significant differences from those generated by the standard HIV/AIDS model proposed by [2,48] for classical derivatives. Across all figures, dynamics reach a steady state as the fractional order decreases from 1 to 0.80 or lower, indicating that

smaller fractional values lead to more efficient solutions. The study's numerical scheme accurately captures the system's dynamics, with each solution approaching a steady-state boundary. These variables exhibit relationships with fluctuating fractional order α and fractal dimension β, demonstrating the influence of fractal features on the dynamics. Such features are absent in integer-order derivatives, highlighting the impact of utilizing fractal-fractional approaches for epidemic models. The findings suggest that slight changes in fractal dimensions and fractional orders only manifest in numerical simulations, with solutions for all compartments achieving the required accuracy and reliability as fractional values decrease. This underscores the effectiveness of fractal-fractional systems, compared to fractional systems [49], in investigating epidemic models and predicting asymptotic behavior around endemic equilibrium.

The fractional operator utilized in the study satisfies all the required theoretical conditions for the considered model, with the parameters demonstrating a substantial influence on the ecological system's stability. Even a slight variation in fractal-fractional orders causes a minor change in the model's behavior, highlighting the importance of fractional derivatives in capturing complex HIV transmission dynamics and enhancing the validity and applicability of the findings compared to classical derivatives. Furthermore, the study emphasizes the system's long-term memory effect, as fractional derivatives exhibit a decrease when the fractional order α approaches 1, further enhancing the accuracy and realism of the suggested HIV disease model. In summary, our considered fractal-fractional order HIV epidemic model offers significant advantages, being more realistic, effective, and efficient than the classical model by improving precision through increased flexibility, resulting in better outcomes. By considering long-term dependencies, non-local impacts, persistence, and recurrence, the model provides valuable insights into HIV transmission dynamics, aiding the public health sector in curbing the disease's spread. Simulations also offer relevant data on how infected patients' circumstances evolve over time, supporting informed decision-making. The study also proposes effective strategies to reduce HIV spread and anticipates future developments in this critical field.

7. Conclusions

Mathematical modeling is instrumental in understanding and managing infectious diseases like HIV. In contrast to classical models, nonlinear compartmental models offer a more nuanced view of disease spread. Our study presents a nonlinear deterministic mathematical model incorporating fractal-fractional order derivatives, specifically in the Caputo sense, to capture HIV infection dynamics. This model integrates three infection levels and delineates transitions between various stages for infected individuals, dividing the population into five compartments. We highlight the model's memory effect, which enriches the understanding of disease spread by incorporating fractional derivatives. To validate the model, we conducted a thorough analysis establishing the existence and uniqueness of solutions using fixed-point methods. Ulam-Hyer's stability was assessed through nonlinear functional analysis, affirming the stability of the model's solutions. Numerical solutions were obtained using the fractal-fractional Adam Bashforth iterative scheme in fractional order, validated through MATLAB simulations. Our numerical simulations explored a range of fractional orders and fractal dimensions, revealing how these parameters influence the model's dynamics. Comparisons with integer-order models were made to evaluate stability and convergence, showing the impact of arbitrary order parameters on model dynamics. Overall, utilizing fractal-fractional derivatives enhances the realism of modeling complex events like HIV spread.

The graphical results further illustrate how variations in fractional orders and fractal dimensions impact the dynamics of HIV spread. The analysis reveals that susceptibility dynamics exhibit an initial decline followed by stabilization, with all compartments of the model converging to the true endemic equilibrium point. Higher fractional orders suggest a more intricate interplay of factors affecting susceptibility, indicating a more efficient utilization of historical data or long-term memory in the transmission process. The

infected populations at stages 1 and 2 show rapid growth as the fractional order α increases, followed by a decline as the fractional order decreases, leading each solution towards a steady-state boundary. Conversely, populations under treatment exhibit a gradual decline as fractional orders increase, emphasizing the sensitivity of dynamics to parameter settings. Additionally, the recovered population increases rapidly with lower fractional orders and declines more noticeably with higher fractional orders. In all figures, the dynamics reach a steady state as the fractional order decreases from 1 to 0.80 or lower, suggesting that smaller fractional values lead to more efficient solutions. Reducing fractional values enhances the accuracy and reliability of solutions across all compartments. This observation highlights the importance of fractal-fractional derivatives in capturing the complex dynamics of HIV transmission, providing more valid and applicable findings compared to fractional and integer order derivatives. The results emphasize the significance of regulating the effective transmission rate to mitigate fatalities, contain HIV transmission, and increase the number of recoveries. Overall, the proposed novel fractal-fractional derivative technique offers more precise measures and may be better suited for deciphering complex phenomena compared to fractional and integer-order operators.

Our research yields invaluable insights for future scientific endeavors. The use of fractal-fractional derivatives uncovers intricate dynamics in viral disease models, surpassing the capabilities of integer-order derivatives. Mathematical modeling encapsulates certain physical phenomena where the classical derivative only captures dynamics in one direction, whereas the fractional operator enables continuous monitoring of infectious diseases. The fractional order allows analysis of infection from its initial point when infected individuals first carry the infection and begin spreading it, until its culmination. This comprehensive approach aids in understanding the complete behavior of infection and the impact of control strategies through modeling. It enhances our comprehension of the disease's complexities and improves predictions of its behavior over time. This analytical approach is instrumental in future research and control plans aimed at mitigating the effects of the disease. It contributes significantly to HIV transmission management and community-level understanding. Future directions include optimizing control strategies, integrating behavioral dynamics into the model with real-world data validation, exploring the application of fractal-fractional derivatives in neural networks, and enhancing the numerical framework by incorporating fractional dimensions into the independent variable ξ. These efforts hold promise in improving the model's applicability and robustness in capturing the dynamics of HIV transmission.

Author Contributions: All authors made equal contributions to the writing of this paper. All authors have accepted responsibility for the entire content of this manuscript and approved its submission. Conceptualization, R.T.A. and Y.N.A.; methodology, N.H.A. and R.T.A.; software, Y.N.A.; validation, N.H.A., Y.N.A. and R.T.A.; formal analysis, S.T.; investigation, R.T.A.; resources, N.H.A. and R.T.A.; writing—original draft preparation, Y.N.A.; review and editing, R.T.A., Y.N.A., N.H.A. and S.T.; visualization, N.H.A. and Y.N.A.; supervision, R.T.A.; project administration, R.T.A.; funding acquisition, N.H.A. and R.T.A. All authors have read and agreed to the published version of the manuscript.

Data Availability Statement: No new data have been created for this study.

Conflicts of Interest: The authors declare no conflict of interest.

References

1. Anderson, R.M. The role of mathematical models in the study of HIV transmission and the epidemiology of AIDS. *J. Acquir. Immune Defic. Syndr.* **1988**, *1*, 241–256. [PubMed]
2. Sakkoum, A.; Lhous, M.; Magri, E.M. A mathematical simulation and optimal control of a VIH model with different infectious level. *J. Math. Comput. Sci.* **2022**, *12*, 117.

3.   Anderson, R.M.; Blythe, S.P.; Gupta, S.; Konings, E. The transmission dynamics of the human immunodeficiency virus type 1 in the male homosexual community in the United Kingdom: The influence of changes in sexual behaviour. *Philos. Trans. R. Soc. Lond. B Biol. Sci.* **1989**, *325*, 45–98. [PubMed]

4.   Nisar, K.S.; Farman, M.; Abdel-Aty, M.; Cao, J. A review on epidemic models in sight of fractional calculus. *Alex. Eng. J.* **2023**, *75*, 81–113. [CrossRef]

5.   Chen, Y.; Liu, F.; Yu, Q.; Li, T. Review of fractional epidemic models. *Appl. Math. Model.* **2021**, *97*, 281–307. [CrossRef]

6.   Ngina, P.; Mbogo, R.W.; Luboobi, L.S. Modelling optimal control of in-host HIV dynamics using different control strategies. *Comput. Math. Methods Med.* **2018**, *2018*, 9385080. [CrossRef] [PubMed]

7.   Silva, C.J.; Torres, D.F. Modeling and optimal control of HIV/AIDS prevention through PrEP. *Discret. Contin. Dyn. Syst.-S* **2018**, *11*, 119–141. [CrossRef]

8.   Shirazian, M.; Farahi, M.H. Optimal control strategy for a fully determined HIV model. *Intell. Control. Autom.* **2010**, *1*, 15–19. [CrossRef]

9.   Li, Z.; Teng, Z.; Miao, H. Modeling and control for HIV/AIDS transmission in China based on data from 2004 to 2016. *Comput. Math. Methods Med.* **2017**, *2017*, 8935314. [CrossRef]

10. Shen, M.; Xiao, Y.; Rong, L. Global stability of an infection-age structured HIV-1 model linking within-host and between-host dynamics. *Math. Biosci.* **2015**, *263*, 37–50. [CrossRef]

11. Shi, S.; Nguyen, P.K.; Cabral, H.J.; Diez-Barroso, R.; Derry, P.J.; Kanahara, S.M.; Kumar, V.A. Development of peptide inhibitors of HIV transmission. *Bioact. Mater.* **2016**, *1*, 109–121. [CrossRef] [PubMed]

12. Huo, H.F.; Chen, R.; Wang, X.Y. Modelling and stability of HIV/AIDS epidemic model with treatment. *Appl. Math. Model.* **2016**, *40*, 6550–6559. [CrossRef]

13. Zhai, X.; Li, W.; Wei, F.; Mao, X. Dynamics of an HIV/AIDS transmission model with protection awareness and fluctuations. *Chaos Solitons Fractals* **2023**, *169*, 113224. [CrossRef]

14. Zafar, Z.U.A.; Ali, N.; Younas, S.; Abdelwahab, S.F.; Nisar, K.S. Numerical investigations of stochastic HIV/AIDS infection model. *Alex. Eng. J.* **2021**, *60*, 5341–5363. [CrossRef]

15. Wang, J.; Zhang, R.; Kuniya, T. Global dynamics for a class of age-infection HIV models with nonlinear infection rate. *J. Math. Anal. Appl.* **2015**, *432*, 289–313. [CrossRef]

16. Singh, R.; Ali, S.; Jain, M. Epidemic model of HIV/AIDS transmission dynamics with different latent stages based on treatment. *Am. J. Appl. Math.* **2016**, *4*, 222–234. [CrossRef]

17. Alyobi, S.; Jan, R. Qualitative and quantitative analysis of fractional dynamics of infectious diseases with control measures. *Fractal Fract.* **2023**, *7*, 400. [CrossRef]

18. Anjam, Y.N.; Yavuz, M.; ur Rahman, M.; Batool, A. Analysis of a fractional pollution model in a system of three interconnecting lakes. *AIMS Biophys.* **2023**, *10*, 220–240. [CrossRef]

19. Qureshi, S.; Atangana, A. Fractal-fractional differentiation for the modeling and mathematical analysis of nonlinear diarrhea transmission dynamics under the use of real data. *Chaos Solitons Fractals* **2020**, *136*, 109812. [CrossRef]

20. Anjam, Y.N.; Shahid, I.; Emadifar, H.; Arif Cheema, S.; ur Rahman, M. Dynamics of the optimality control of transmission of infectious disease: A sensitivity analysis. *Sci. Rep.* **2024**, *14*, 1041. [CrossRef]

21. Anjam, Y.N.; Shafqat, R.; Sarris, I.E.; Ur Rahman, M.; Touseef, S.; Arshad, M. A fractional order investigation of smoking model using Caputo-Fabrizio differential operator. *Fractal Fract.* **2022**, *6*, 623. [CrossRef]

22. Caputo, M.; Fabrizio, M. On the singular kernels for fractional derivatives. Some applications to partial differential equations. *Progr. Fract. Differ. Appl.* **2021**, *7*, 79–82.

23. Caputo, M.; Fabrizio, M. A new definition of fractional derivative without singular kernel. *Prog. Fract. Differ. Appl.* **2015**, *1*, 73–85.

24. Atangana, A. Fractal-fractional differentiation and integration: Connecting fractal calculus and fractional calculus to predict complex system. *Chaos Solitons Fractals* **2017**, *102*, 396–406. [CrossRef]

25. ur Rahman, M.; Ahmad, S.; Matoog, R.T.; Alshehri, N.A.; Khan, T. Study on the mathematical modelling of COVID-19 with Caputo-Fabrizio operator. *Chaos Solitons Fractals* **2021**, *500*, 111121. [CrossRef]

26. Zhang, T.; Zhao, Y.; Xu, X.; Wu, S.; Gu, Y. Solution and dynamics analysis of fractal-fractional multi-scroll Chen chaotic system based on Adomain decomposition method. *Chaos, Solitons Fractals* **2024**, *178*, 114268. [CrossRef]

27. Almutairi, N.; Saber, S. Application of a time-fractal fractional derivative with a power-law kernel to the Burke-Shaw system based on Newton's interpolation polynomials. *MethodsX* **2024**, *12*, 102510. [CrossRef] [PubMed]

28. Asifa; Anwar, T.; Kumam, P.; Sitthithakerngkiet, K.; Muhammad, S. A fractal-fractional model-based investigation of shape influence on thermal performance of tripartite hybrid nanofluid for channel flows. *Numer. Heat Transf. Part A Appl.* **2024**, *85*, 155–186. [CrossRef]

29. Adom-Konadu, A.; Bonyah, E.; Sackitey, A.L.; Anokye, M.; Asamoah, J.K.K. A fractional order Monkeypox model with protected travelers using the fixed point theorem and Newton polynomial interpolation. *Healthc. Anal.* **2023**, *3*, 100191. [CrossRef]

30. Atangana, A.; Qureshi, S. Modeling attractors of chaotic dynamical systems with fractal–fractional operators. *Chaos Solitons Fractals* **2019**, *123*, 320–337. [CrossRef]

31. Li, Z.; Liu, Z.; Khan, M.A. Fractional investigation of bank data with fractal-fractional Caputo derivative. *Chaos Solitons Fractals* **2020**, *131*, 109528. [CrossRef]

32. Owolabi, K.M.; Shikongo, A. Fractal fractional operator method on HER2+ breast cancer dynamics. *Int. J. Appl. Comput. Math.* **2021**, *7*, 85. [CrossRef]

33. Ahmad, S.; Ullah, A.; Abdeljawad, T.; Akgül, A.; Mlaiki, N. Analysis of fractal-fractional model of tumor-immune interaction. *Results Phys.* **2021**, *25*, 104178. [CrossRef]

34. Anjam, Y.N.; Arshad, A.; Alqahtani, R.T.; Arshad, M. Unveiling the dynamics of drug transmission: A fractal-fractional approach integrating criminal law perspectives. *AIMS Math.* **2024**, *9*, 13102–13128. [CrossRef]

35. Liu, X.; ur Rahmamn, M.; Ahmad, S.; Baleanu, D.; Nadeem Anjam, Y. A new fractional infectious disease model under the non-singular Mittag–Leffler derivative. *Waves Random Complex Media* **2022**, 1–27. [CrossRef]

36. Ali, Z.; Rabiei, F.; Shah, K.; Khodadadi, T. Qualitative analysis of fractal-fractional order COVID-19 mathematical model with case study of Wuhan. *Alex. Eng. J.* **2021**, *60*, 477–489. [CrossRef]

37. Qureshi, S.; Rangaig, N.A.; Baleanu, D. New numerical aspects of Caputo-Fabrizio fractional derivative operator. *Mathematics* **2019**, *7*, 374. [CrossRef]

38. Atangana, A. Modelling the spread of COVID-19 with new fractal-fractional operators: Can the lockdown save mankind before vaccination? *Chaos Solitons Fractals* **2020**, *136*, 109860. [CrossRef] [PubMed]

39. Farman, M.; Sarwar, R.; Akgul, A. Modeling and analysis of sustainable approach for dynamics of infections in plant virus with fractal fractional operator. *Chaos Solitons Fractals* **2023**, *170*, 113373. [CrossRef]

40. Granas, A.; Dugundji, J. *Fixed Point Theory*; Springer: New York, NY, USA, 2003; Volume 14, pp. 15–16.

41. Kongson, J.; Sudsutad, W.; Thaiprayoon, C.; Alzabut, J.; Tearnbucha, C. On analysis of a nonlinear fractional system for social media addiction involving Atangana-Baleanu-Caputo derivative. *Adv. Differ. Equ.* **2021**, *2021*, 356. [CrossRef]

42. Kreyszig, E. *Introductory Functional Analysis with Applications*; John Wiley Sons: Hoboken, NJ, USA, 1991; Volume 17.

43. Huo, H.F.; Feng, L.X. Global stability for an HIV/AIDS epidemic model with different latent stages and treatment. *Appl. Math. Model.* **2013**, *37*, 1480–1489. [CrossRef]

44. Alizon, S.; Magnus, C. Modelling the course of an HIV infection: Insights from ecology and evolution. *Viruses* **2012**, *4*, 1984–2013. [CrossRef] [PubMed]

45. Yusuf, T.T.; Benyah, F. Optimal strategy for controlling the spread of HIV/AIDS disease: A case study of South Africa. *J. Biol. Dyn.* **2012**, *6*, 475–494. [CrossRef] [PubMed]

46. Arruda, E.F.; Dias, C.M.; de Magalhã, C.V.; Pastore, D.H.; Thomé, R.C.; Yang, H.M. An optimal control approach to HIV immunology. *Appl. Math.* **2015**, *6*, 1115–1130. [CrossRef]

47. Kumar, S.; Chauhan, R.P.; Osman, M.S.; Mohiuddine, S.A. A study on fractional HIV-AIDs transmission model with awareness effect. *Math. Methods Appl. Sci.* **2023**, *46*, 8334–8348. [CrossRef]

48. Cai, L.; Li, X.; Ghosh, M.; Guo, B. Stability analysis of an HIV/AIDS epidemic model with treatment. *J. Comput. Appl. Math.* **2009**, *229*, 313–323. [CrossRef]

49. Khan, A.; Gómez-Aguilar, J.F.; Khan, T.S.; Khan, H. Stability analysis and numerical solutions of fractional order HIV/AIDS model. *Chaos Solitons Fractals* **2019**, *122*, 119–128. [CrossRef]